



Defect assessment of Mg-doped GaN by beam injection techniques

C. Díaz-Guerra, J. Piqueras, A. Castaldini, A. Cavallini, and L. Polenta

Citation: *J. Appl. Phys.* **94**, 7470 (2003); doi: 10.1063/1.1628832

View online: <http://dx.doi.org/10.1063/1.1628832>

View Table of Contents: <http://jap.aip.org/resource/1/JAPIAU/v94/i12>

Published by the [AIP Publishing LLC](#).

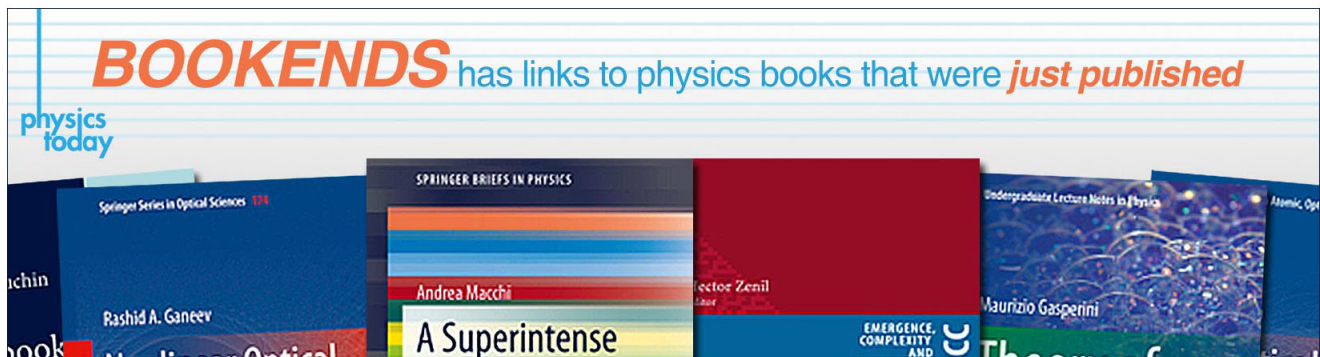
Additional information on *J. Appl. Phys.*

Journal Homepage: <http://jap.aip.org/>

Journal Information: http://jap.aip.org/about/about_the_journal

Top downloads: http://jap.aip.org/features/most_downloaded

Information for Authors: <http://jap.aip.org/authors>



Defect assessment of Mg-doped GaN by beam injection techniques

C. Díaz-Guerra^{a)} and J. Piqueras

Departamento de Física de Materiales, Facultad de Físicas, Universidad Complutense, Ciudad Universitaria s/n, E-28040 Madrid, Spain

A. Castaldini, A. Cavallini, and L. Polenta

INFM and Dipartimento di Fisica, Università di Bologna, INFM, Viale Berti Pichat 6/2, I-40127 Bologna, Italy

(Received 14 July 2003; accepted 2 October 2003)

The electronic recombination properties of Mg-doped GaN have been investigated by steady state and time-resolved cathodoluminescence (TRCL) in the scanning electron microscope, photocurrent (PC) spectroscopy, and optical beam induced current (OBIC). CL and OBIC maps reveal an inhomogeneous recombination activity in the investigated material. Deep levels giving rise to level-to-band transitions were detected by PC spectroscopy. A large PC quenching observed upon illumination with light of (2.65–2.85) eV is tentatively attributed to metastable traps within the band gap. CL spectra reveal the existence of emission bands centered at 85 K at 3.29, 3.20, 3.15, and 3.01 eV, respectively. Both time-resolved and steady-state CL measurements carried out under different excitation conditions indicate that the 3.15 and 3.01 eV emissions are likely related to donor-acceptor pair transitions. TRCL measurements also reveal different recombination kinetics for these bands and suggest that deep donors are involved in the mechanism responsible for the 3.01 eV emission. © 2003 American Institute of Physics. [DOI: 10.1063/1.1628832]

I. INTRODUCTION

Gallium nitride has become one of the most promising semiconductors for optoelectronics and high power/high temperature applications. In this context, good quality *p*-type GaN is one of the key requirements in developing high-performance devices.¹ However, compensation of acceptors is still a serious problem in nitrides technology while it is also recognized that a better understanding of the influence of deep level defects on the electronic and optical properties of GaN is necessary in order to improve devices design.^{1,2} On the other hand, standard growth of *p*-type GaN makes use of epitaxial techniques on sapphire and SiC substrates. Mismatch-induced lattice strain causes the formation of extended defects, mainly dislocations, which create a highly degenerate layer at the GaN/sapphire interface³ and partially propagate in the growth direction.²

Several electron and optical beam injection techniques have been applied to study gap states in GaN. Cathodoluminescence (CL) in the scanning electron microscope (SEM) has been previously used to obtain information on the spatial distribution of the different emission bands and their association to extended defects, e.g., Refs. 4 and 5. However, time-resolved cathodoluminescence (TRCL) has been mainly used to investigate relaxation kinetics of charge carriers in GaN-based quantum heterostructures.⁶ Another spectroscopic technique, spectrally resolved photocurrent (PC), has been recently applied to the study of trapping processes in GaN.^{7,8} As compared with CL, that evidences radiative internal and band-to-level transitions, PC allows us to detect both radiative and nonradiative band-to-level transitions. A further use-

ful technique for semiconductor characterization, charge-collection optical scanning microscopy, has been scarcely employed in defect assessment of this wide band gap semiconductor.⁹ In the present work, TRCL in the SEM, optical beam induced current (OBIC) microscopy and PC spectroscopy are used as a set of complementary techniques to study the recombination kinetics and the electrical and optical properties of the defect structure of Mg-doped GaN. In particular, the homogeneity of the recombination activity and the origin of deep level related transitions—detected by PC and CL under different excitations conditions—have been investigated.

II. EXPERIMENT

Mg-doped GaN, 1.8- μm -thick, grown by molecular beam epitaxy (MBE) on sapphire was investigated in this work. Room temperature capacitance–voltage and Hall measurements respectively indicate a free carrier concentration of $p = 1 \times 10^{17} \text{ cm}^{-3}$ and a mobility of $\mu_h = 15 \text{ cm}^2/\text{V s}$.

CL observations were carried out in a Hitachi S-2500 SEM. Measurements were performed at accelerating voltages ranging from 5 to 20 kV and temperatures between 85 and 295 K. One of the main topics addressed by previous CL studies of Mg-doped GaN was the evolution of luminescence spectral distribution with electron beam irradiation time and its possible relation with dissociation of Mg–H complexes.^{10,11} In the present study, a global increase of the CL emission with increasing irradiation time was also detected, but no change in the relative intensities of the observed spectral features was found. Such overall intensity increase saturated after 5–10 min of continuous irradiation, depending on the excitation conditions. CL spectra presented in this work were recorded after the mentioned saturation

^{a)}Electronic mail: cdiazguerra@fis.ucm.es

state was reached. Steady-state CL spectra were acquired using a charge coupled device camera with a built-in spectrograph (Hamamatsu PMA-11). For time-resolved measurements a periodic beam was generated using a graphite chopper and beam-blanking electronics. To record CL spectra at different delay times the signal from a photomultiplier was collected by a boxcar integrator triggered by a pulse generator, and then fed to a computer (see Ref. 12 for further details). TRCL spectra were measured at delay times ranging from 1 μs to 5 ms with time windows between 500 ns and 500 μs . The intensities of the different CL emissions as a function of the excitation pulse width were monitored with the aid of a digital oscilloscope.

In order to perform PC and OBIC measurements, semi-transparent Schottky diodes 200 Å thick were deposited on the film by Au evaporation, while ohmic contacts were prepared using an eutectic Ga–Al alloy. These experiments were performed at room temperature using the experimental setup described in Ref. 13 with a beam light diameter of 5 μm . In spectral photocurrent analyses the light wavelength was changed from 320 to 650 nm (3.88 to 1.91 eV). The monochromator slit widths were properly adjusted in order to maximize resolution of PC spectra obtained under different bias conditions. CL and PC spectra were corrected for the optical response of the systems used. OBIC scanning microscopy was carried out illuminating the sample with a 352 nm (3.52 eV) light.

III. RESULTS AND DISCUSSION

The film shows a featureless surface in the SEM secondary electron mode observations. On the contrary, SEM–CL images [Fig. 1(a)] reveal an inhomogeneous luminescence spatial distribution, showing a granular contrast pattern in which the smallest observed features are of the order of 0.4 μm . Efficient CL emission is observed in areas of up to about 35 μm^2 in size. No contrast changes have been observed by increasing the electron beam accelerating voltage while keeping a constant beam power, which suggests a uniform in-depth distribution of the radiative recombination centers. In addition, no microcracks or large optically dead areas have been found. OBIC mapping [Fig. 1(b)] shows a black/white contrast related to the defect distribution very similar to that observed by panchromatic CL, although the spatial resolution is lower due to the large light beam spot size. These CL and OBIC contrasts were observed regardless the investigated area of the material. Dark OBIC contrast is related to both nonradiative and radiative recombination processes, thus, the similarity of OBIC and CL patterns suggests that the dark OBIC contrast is related to nonradiative recombination.¹⁴

Steady state CL spectra show luminescence emission in the (2.6–3.5) eV spectral range (Fig. 2). The spectral distribution of the CL was found to be homogeneous throughout the investigated material. No emission in the green or yellow range of the visible spectrum was detected at low (85 K) or room temperature. In order to evidence a possible thickness dependence of the distribution of the radiative centers involved in the observed luminescence bands, depth-resolved

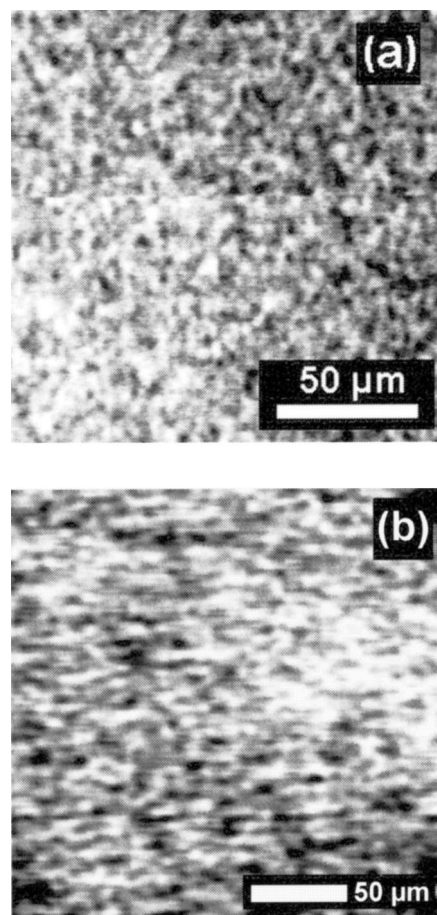


FIG. 1. (a) Panchromatic CL image (12 kV, 5 nA, 88 K) of a GaN:Mg film. (b) Room temperature OBIC image of the same sample obtained illuminating the film with a 352 nm light.

CL measurements were performed by varying the beam accelerating voltage (V_b) while using a constant electron-hole pair injection rate, i.e., keeping a constant electron beam power ($I_b V_b$). In this way, real inhomogeneities in the in-

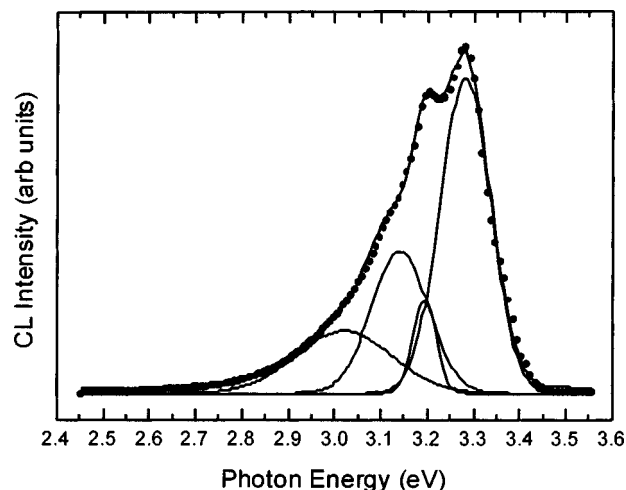


FIG. 2. Gaussian deconvolution of a low temperature (85 K) CL spectrum (12 kV, 5 nA). Emission bands are found centered at 3.29, 3.20, 3.15, and 3.01 eV. Circles represent the experimental data while the upper solid line corresponds to the best-fit curve.

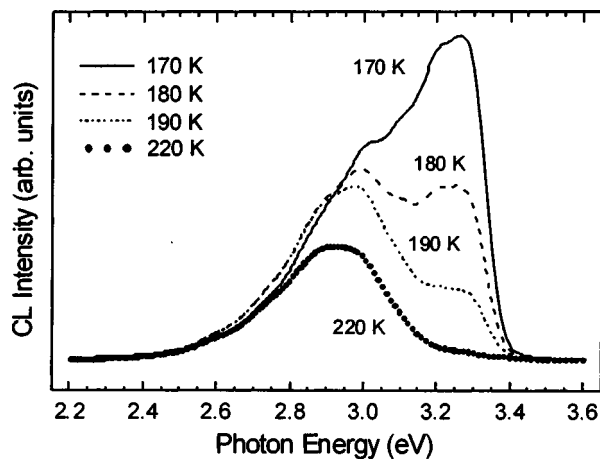


FIG. 3. CL spectra (12 kV, 5 nA) recorded at different temperatures in the interval where the spectral distribution of the emission shows pronounced changes in the dominant band.

depth distribution of recombining defect centers can be distinguished from effects due to unequal carrier injection conditions. It was found that the relative intensities of the emission bands appearing in steady-state CL spectra were independent of the accelerating voltage used, which evidences that the defect centers responsible for the luminescence emissions are uniformly distributed throughout the sample. Such observations were confirmed by CL measurements carried out in cross-section configuration.

Gaussian deconvolution of the spectra obtained at 85 K reveals the existence of four CL bands centered at this temperature at about 3.29, 3.20, 3.15, and 3.01 eV (Fig. 2). The same peak positions are found by deconvolution of other CL spectra recorded either in planar or cross-section configuration. The 3.29 eV emission, with its phonon replica at 3.20 eV, has been attributed in Mg-doped GaN either to a shallow donor-acceptor pair (DAP) transition¹⁵ or to a free electron-to-acceptor transition (e^0-A).¹⁶ No energy shift of this peak was observed in the present work when the excitation density was varied, which agrees with the free electron-acceptor transition model. In addition, such emission was found to be the dominant band at 85 K. These observations suggest a rather high degree of compensation in the material here investigated, as supported by the quite low hole concentration measured.¹⁶ This emission is significantly quenched above 200 K due to free hole release rather than to acceptors thermal ionization.¹⁷ Figure 3 presents CL spectra obtained in the temperature interval where the gradual quenching of the free electron-acceptor transition takes place and the lower energy CL bands become the dominant emissions. It was found that the bands centered at 3.15 and 3.01 eV at 85 K strongly shift to lower energies by increasing temperature. At 180 K, these emissions appear centered at 3.06 and 2.92 eV, while at 280 K they appear respectively peaked at 2.92 and 2.76 eV, giving rise to the broadband centered at 2.86 eV shown in Fig. 4. In addition, the width of such emissions increases when temperature is raised. Full widths at medium height (FWMH) of 150 and 225 meV were, respectively, found at 85 K for the 3.15 and 3.01 eV CL bands, while at 280 K FWHM values of 290 and 395 meV were measured for the

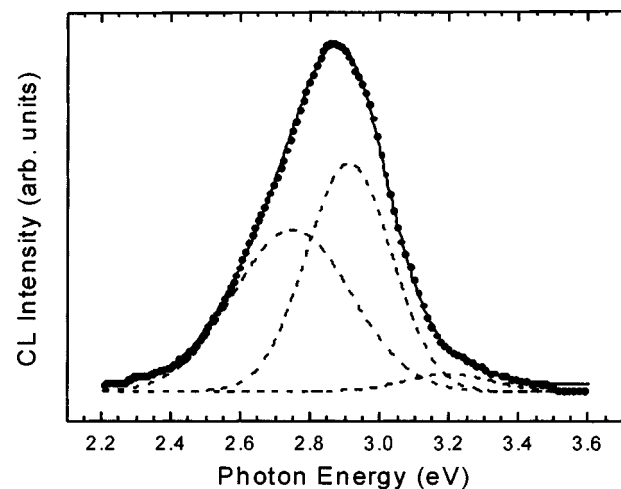


FIG. 4. Gaussian deconvolution of a room temperature (280 K) CL spectrum (12 kV, 5 nA). Emission bands are found centered at 3.22, 2.92, and 2.76 eV (dashed lines). The solid line corresponds to the best-fit curve while circles represent experimental data.

mentioned emissions. These values are similar to the ones previously observed in photoluminescence (PL) experiments by Sheu *et al.*¹⁶ and Reshchikov *et al.*¹⁸

A PL band centered at 3.1–3.2 eV has been related in MBE-grown GaN:Mg to shallow acceptors.¹⁷ However, the origin of the 3.01 eV band remains unclear. Different models have been proposed to explain the so-called blue luminescence of Mg-doped GaN. This emission has been often attributed to a DAP transition involving a deep level, but there has been no consensus as to whether the deep defect is a deep donor^{18,19} or a deep acceptor.¹⁶ The temperature redshift of the blue GaN:Mg band observed in this work agrees with the proposed DAP nature of the emission. Under the high CL excitation conditions, the Coulomb interaction between close pairs is strong and the resultant ionization energy decreases enough for thermal release of charge carriers. As a result, the high-energy portion of the spectrum begins quenching at lower temperatures and the band is redshifted. Nevertheless, it should be mentioned that transitions from the conduction band to a deep acceptor²⁰ or transitions from a deep donor to the valence band²¹ have also been proposed to explain the blue emission. We will further address this point when discussing our TRCL data.

PC measurements reveal the existence of traps in spectral ranges where no CL emission was detected under any excitation conditions. Besides the peak centered at about 3.45 eV, related to the band gap excitation, two other peaks are observed at 2.39 and 2.29 eV (Fig. 5). Transitions in the green-yellow range are rarely observed in *p*-type GaN films. It has been often suggested^{21,22} that the yellow luminescence band is present in *n*-type GaN due to the existence of gallium vacancies or gallium vacancies complexes. In the frame of this model, Mg atoms compensate the V_{Ga} in Mg-doped GaN²³ and therefore the yellow emission decreases even if it does not always completely disappear. Salviati *et al.*²⁴ observed CL emission at 2.2 eV in MBE grown *p*-type GaN and proposed a transition between a deep N_{Ga} donor and a shallow Mg_{Ga} acceptor as the mechanism responsible for the

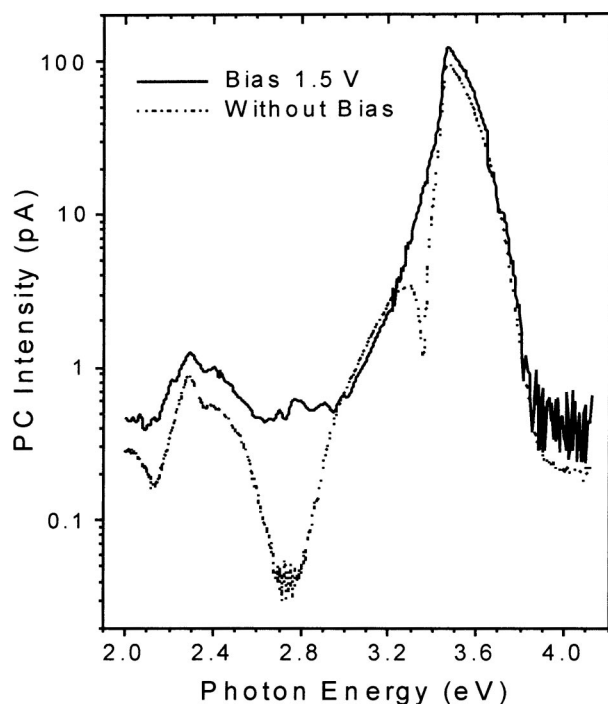


FIG. 5. Photocurrent spectra of a Mg-doped film recorded at room temperature without applied reverse bias (dashed line) and applying a 1.5 V reverse bias (solid line).

observed luminescence. Yellow PL, attributed to Mg–O complexes, has also been occasionally observed in GaN bulk crystals.²⁵ Whatever their nature is, observation of the 2.39 and 2.29 eV peaks in our PC spectra but not in CL measurements carried out at different temperatures and excitation densities suggests that the mentioned peaks are related to defects giving rise to nonradiative transitions.

Another PC peak is observed centered at 3.30 eV. A peak at the same energy has been previously observed²⁶ in PC spectra of Mg-doped GaN films and attributed to a transition from a Mg shallow acceptor level to the conduction band. This level, located (130–170) meV above the valence band, has been also detected by Hall effect and admittance spectroscopy measurements.^{27,28} Our 3.30 eV PC peak broadens by applying an external bias, maybe due to potential fluctuations typical in compensated GaN:Mg. Actually, the band is no more observed as a resolved peak when a reverse bias higher than 1 V is applied.

Spectra presented in Fig. 5 also show how upon illumination with light of (2.65–2.85) eV the photocurrent decreases below the dark current value when no bias voltage is applied to the sample, i.e., when current is just collected by the built-in voltage. This PC quenching is maximum at about 2.75 eV. Interestingly, the mentioned energy range coincides with the interval where luminescence emission has been observed in Mg-doped GaN films by CL and PL in this and other works.^{19,29,30} Optical quenching of the photoconductivity and the persistent photoconductivity has been previously observed in *n*-type material GaN.^{7,31} Models proposed to account for these effects usually invoke the existence of metastable traps for minority carriers or the interplay between deep traps and recombination centers within the band gap. In

our case, the existence of a metastable electron trap located 2.75 eV above the valence band (about 0.65 eV below the conduction band) would explain the decrease of the PC level below the dark current level. Upon illumination with light of the same energy as the electron trap, a change in the electronic configuration of the defect related to the trap takes place, e.g., due to a change in the charge state of the defect or to a lattice relaxation to a more stable configuration. Electrons may then escape from this trap and recombine radiatively with valence band holes. This would lower the free hole concentration leading to the observed dark current decrease. Theoretical studies³² indicate that Mg_{*i*}–V_N complexes with different charge states may introduce defect levels in the band gap—clustered at around 2.8 eV above the valence band maximum—related to different lattice relaxations of the neighboring Ga atoms. Besides, an energy barrier of about 1.4 eV was calculated for Mg migration from the complexes to the nearest interstitial sites. Our experimental results show that photocurrent quenching is suppressed applying a 1.5 V bias voltage to the sample, although a systematic study of the threshold bias necessary to avoid such quenching has not been carried out. It should also be mentioned that the existence of a deep donor at about 0.62 eV below the valence band has been observed by deep level transient spectroscopy in Mg-doped samples.³³

Figure 6(a) shows TRCL spectra recorded at 180 K for a delay time of 1 ms and beam excitation pulses of 3 and 70 μ s. Steady state spectra obtained at the same temperature (Fig. 3) show almost equal intensities for the CL (e^0 –A) emission (3.29 eV) and the CL bands observed at lower energies (3.06 and 2.92 eV). On the contrary, TRCL spectra presented in Fig. 6 show these low energy bands as the dominant emissions. Gaussian deconvolution of the TRCL spectrum recorded after excitation with 3 μ s pulses [Fig. 6(b)] shows the mentioned bands centered at 3.02 and 2.82 eV, i.e., redshifted as compared with the steady state spectrum recorded at the same temperature. In addition, the overall emission appears to further redshift when the excitation pulse width is increased from 3 to 70 μ s. However, deconvolution of several TRCL spectra recorded after excitation with 70 μ s pulses indicate that this apparent shift is actually due to the intensity increase of the 2.82 eV component relative to the 3.02 eV band. This is confirmed by measurements of the intensity of both CL bands as a function of the excitation beam pulse width (Fig. 7). The experimental data are well fitted by the following empirical law:

$$I_{CL} = I_s [1 - \exp(-t/\tau_f)] \quad (1)$$

I_s represents the CL intensity in the quasisteady state and τ_f —the key parameter providing information on the recombination kinetics—is the time for the CL intensity to reach a factor $(1 - 1/e)$ of I_s . It is clearly appreciated that a quasisteady state condition is not reached for any of these emissions with pulses shorter than about 450 μ s. Results obtained after fitting our data to Eq. (1) give τ_f values of (162 ± 8) μ s and (109 ± 5) μ s for the 2.92 and 3.06 eV bands, respectively (Fig. 7). The slower intensity raise of the 2.92 eV luminescence explains why its relative weight in the total emission

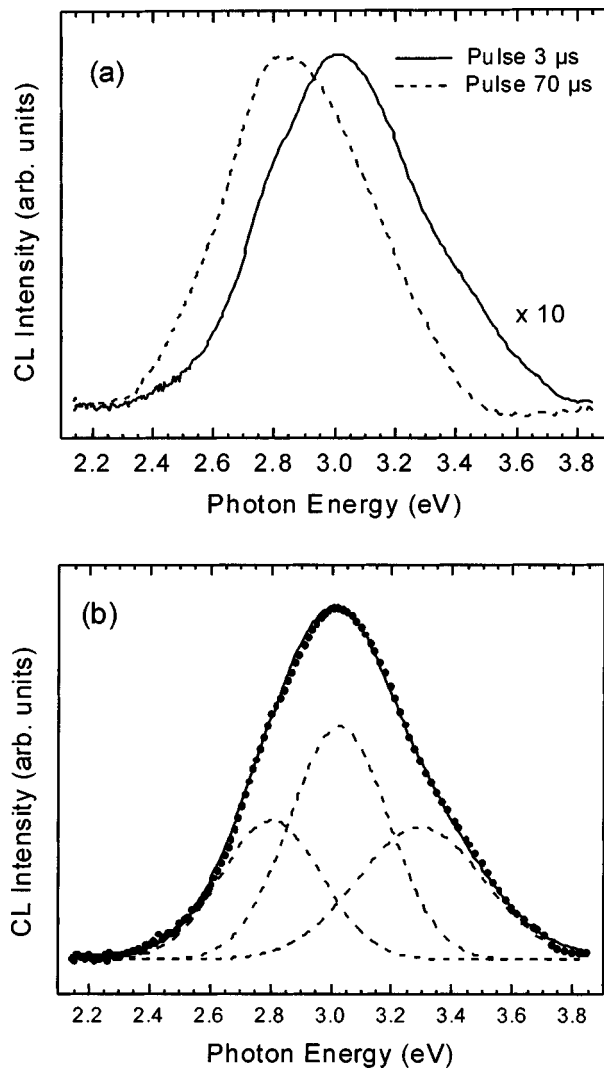


FIG. 6. (a) Normalized TRCL spectra (15 kV, 10 nA) measured at 180 K for a 1 ms delay time using a 3 μs electron beam excitation pulse (solid line) and a 70 μs excitation pulse (dashed line). (b) Gaussian deconvolution of the CL spectrum recorded with a 3 μs pulse. Emission bands are centered at 3.28, 3.02, and 2.82 eV (dashed lines). The solid line is the best-fit curve while circles correspond to experimental data.

increases by increasing the electron pulse width, shifting the overall CL maximum towards lower energies [Fig. 6(a)].

As discussed before, our steady state measurements carried out at different temperatures supported the DAP nature of the CL emission bands centered at 180 K at 3.06 and 2.92 eV. TRCL measurements agree with this possibility as well. The observed redshift of both bands with increasing delay time is due to differences in the Coulomb interactions for close and distant pairs. Pairs with a small separation will emit at higher energies with shorter lifetimes, whereas the more distant pairs emit at lower energy with a longer decay time.³⁴ In particular, the shift of about 100 meV observed for the blue 2.92 eV band is indicative of its deep donor-acceptor transition nature, in agreement with previous time-resolved PL studies.³⁵ The deep donor has been attributed to $\text{Mg}_{\text{Ga}}-\text{V}_{\text{N}}$, $\text{Mg}_{\text{i}}-\text{V}_{\text{N}}$ or $\text{V}_{\text{N}}-\text{H}$ ^{19,32,29} complexes, while the acceptor is likely related to a substitutional Mg_{Ga} defect.^{29,36} Nevertheless, the role of potential fluctuations, characteristic

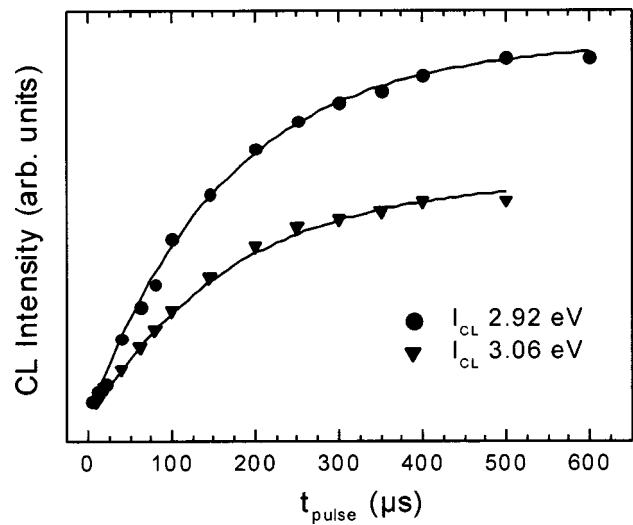


FIG. 7. CL intensity of the bands centered at 180 K at 2.92 and 3.06 eV as a function of the electron excitation pulse width. Solid lines correspond to fits to Eq. (1).

of highly compensated semiconductors, should be also taken into account. Actually, DAP emission and non-DAP emission in the presence of potential fluctuations bear a number of similarities,¹⁸ and it can be difficult to distinguish which one of these two mechanisms is responsible for the 2.92 eV emission. It was found in this work that a reduction of the electron beam excitation density did not lead to a larger redshift of the mentioned blue CL band. A larger redshift at reduced power density would be observed if the shift were related to potential fluctuations effects, since screening of fluctuations would be reduced due to decreased screening.³⁷ Hence, this observation indicates that potential fluctuations may play only a secondary role on the emission mechanism, that would correspond to a DAP transition. Figure 8 presents an energy scheme showing transitions giving rise to CL and PC defect bands observed in the Mg-doped GaN investigated.

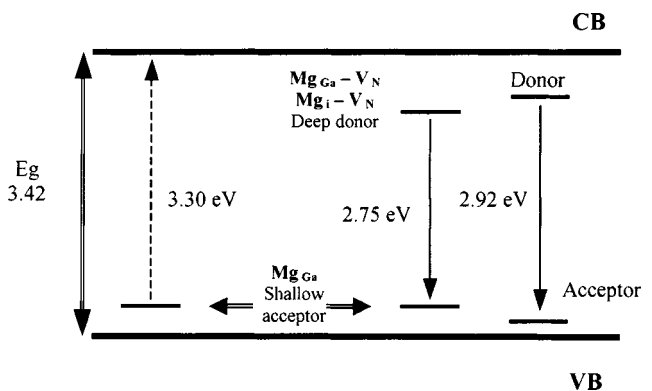


FIG. 8. Energy scheme showing the transitions giving rise to CL (solid arrows) and PC (dotted arrow) defect bands observed in the Mg-doped GaN investigated. The $\text{Mg}_{\text{i}}-\text{V}_{\text{N}}$ deep donor is also involved in the process leading to the PC quenching observed between 2.65 and 2.85 eV. At 85 K, radiative transitions from the conduction band to the Mg_{Ga} shallow donor are responsible for the CL emission centered at 3.29 eV.

IV. CONCLUSIONS

The local optical and electronic properties of Mg-doped GaN have been investigated using CL in the SEM, TRCL, PC spectroscopy, and OBIC microscopy as a set of complementary characterization techniques. CL and OBIC mappings show a highly inhomogeneous recombination activity in the investigated material. PC spectroscopy reveals the existence of deep levels giving rise to nonradiative transitions in the green-yellow range of the visible spectrum, as well as other levels influenced by electric field effects. A strong photocurrent quenching observed upon illumination with light of (2.65–2.85) eV is tentatively attributed to metastable traps within the band gap. Steady-state CL spectra reveal the existence of emission bands centered at 85 K at 3.29, 3.20, 3.15, and 3.01 eV. The behavior of these bands under different excitation conditions has been monitored. CL measurements carried out at several temperatures and excitation densities indicate that the 3.15 and 3.01 eV emissions are likely related to DAP transitions. This is confirmed by TRCL spectra showing a clear redshift of the corresponding peak positions with increasing delay time. TRCL measurements reveal different recombination kinetics for these bands and suggest that deep donors are involved in the mechanism responsible for the 3.01 eV emission.

ACKNOWLEDGMENTS

The authors wish to thank D. C. Look, H. Morkoç, and J. van Nostrand for providing the investigated material. This work has been partially supported by MCYT through Project No. MAT2000-2119.

- ¹S. J. Pearton, F. Ren, A. P. Zhang, and K. P. Lee, *Mater. Sci. Eng.*, R. **30**, 55 (2000).
- ²H. Morkoç, *Mater. Sci. Eng.*, R. **33**, 135 (2001).
- ³D. C. Look and R. J. Molnar, *Appl. Phys. Lett.* **70**, 3377 (1997).
- ⁴F. A. Ponce, D. P. Bour, W. Götz, and P. J. Wright, *Appl. Phys. Lett.* **68**, 57 (1996).
- ⁵M. Herrera Zaldívar, P. Fernández, and J. Piqueras, *J. Appl. Phys.* **83**, 2796 (1998).
- ⁶X. Zhang, D. H. Rich, J. Y. Kobayashi, N. P. Kobayashi, and P. D. Dapkus, *Appl. Phys. Lett.* **73**, 1430 (1998).
- ⁷S. J. Chung, M. S. Jeong, O. H. Cha, C.-H. Hong, E.-K. Shu, H. J. Lee, Y. S. Kim, and B. H. Kim, *J. Appl. Phys.* **89**, 5454 (2001).

- ⁸A. Castaldini, A. Cavallini, L. Polenta, and G. Salviati, *Solid State Phenom.* **78–79**, 95 (2001).
- ⁹C. K. Sun *et al.*, *Opt. Quantum Electron.* **32**, 619 (2000).
- ¹⁰X. Li and J. J. Coleman, *Appl. Phys. Lett.* **69**, 1605 (1996).
- ¹¹Y. Koide, D. E. Walker, B. D. White, L. J. Brillson, M. Murakami, S. Kamiyama, H. Amano, and I. Akasaki, *J. Appl. Phys.* **92**, 3657 (2002).
- ¹²A. Urbietta, P. Fernández, J. Piqueras, Ch. Hardalov, and T. Sekiguchi, *J. Phys. D* **34**, 2945 (2001).
- ¹³A. Castaldini, A. Cavallini, and L. Polenta, *Mater. Res. Soc. Symp. Proc.* **588**, 51 (2000).
- ¹⁴M. Avella, E. de la Puente, J. Jiménez, A. Castaldini, A. Cavallini, and L. Polenta, *J. Cryst. Growth* **210**, 220 (2000).
- ¹⁵A. K. Viswanath, E. Shin, J. I. Lee, S. Yu, D. Kim, B. Kim, Y. Chi, and C. Hong, *J. Appl. Phys.* **83**, 2272 (1998).
- ¹⁶J. K. Sheu, Y. K. Su, G. C. Chi, B. J. Pong, C. Y. Chen, C. N. Huang, and W. C. Chen, *J. Appl. Phys.* **84**, 4590 (1998).
- ¹⁷M. Leroux, N. Grandjean, B. Beaumont, G. Nataf, F. Semond, J. Massies, and P. Gibart, *J. Appl. Phys.* **86**, 3721 (1999).
- ¹⁸M. A. Reshchikov, G.-C. Yi, and B. W. Wessels, *Phys. Rev. B* **59**, 13176 (1999).
- ¹⁹F. Shahedipour and B. W. Wessels, *Appl. Phys. Lett.* **76**, 3011 (2000).
- ²⁰E. Oh, H. Park, and Y. Park, *Appl. Phys. Lett.* **72**, 70 (1998).
- ²¹J. Neugebauer and C. G. Van de Walle, *Appl. Phys. Lett.* **69**, 503 (1996).
- ²²K. Saarinen *et al.*, *Phys. Rev. Lett.* **79**, 3030 (1997).
- ²³C. G. Van de Walle, C. Stampfl, and J. Neugebauer, *J. Cryst. Growth* **189–190**, 505 (1998).
- ²⁴G. Salviati *et al.*, *MRS Internet J. Nitride Semicond. Res.* **5S1**, W11.50 (2000).
- ²⁵M. W. Bayerl *et al.*, *Phys. Rev. B* **63**, 125203 (2001).
- ²⁶S. J. Chung, O. H. Cha, H. K. Cho, M. S. Jeong, C.-H. Hong, E.-K. Suh, and H. J. Lee, *Mater. Res. Soc. Symp. Proc.* **F99**, W11.83 (2000).
- ²⁷W. Götz, N. M. Johnson, J. Walker, D. P. Bour, and R. A. Street, *Appl. Phys. Lett.* **68**, 667 (1996).
- ²⁸J. W. Huang, T. F. Kuech, H. Lu, and I. Bhat, *Appl. Phys. Lett.* **65**, 2392 (1996).
- ²⁹U. Kaufmann, M. Kunzer, H. Obloh, M. Maier, Ch. Manz, A. Ramakrishnan, and B. Santic, *Phys. Rev. B* **59**, 5561 (1999).
- ³⁰M. Herrera Zaldívar, P. Fernández, J. Piqueras, and J. Solís, *J. Appl. Phys.* **85**, 1120 (1999).
- ³¹Z. C. Huang, D. B. Mott, P. K. Shu, R. Zhang, J. C. Chen, and D. K. Wickenden, *J. Appl. Phys.* **82**, 2707 (1997).
- ³²S. G. Lee and K. J. Chang, *Semicond. Sci. Technol.* **14**, 138 (1999).
- ³³P. Hacke, T. Detchprohm, K. Hiramatsu, N. Sawaki, K. Tadatomo, and K. Miyake, *Appl. Phys. Lett.* **68**, 1362 (1996).
- ³⁴G. Thomas, J. J. Hopfield, and W. M. Augustyniak, *Phys. Rev.* **140**, A202 (1965).
- ³⁵F. Shahedipour and B. W. Wessels, *MRS Internet J. Nitride Semicond. Res.* **6**, 12 (2001).
- ³⁶J. M. Myoung, K. H. Shim, C. Kim, O. Gluschenov, K. Kim, S. Kim, D. A. Turnbull, and S. G. Bishop, *Appl. Phys. Lett.* **69**, 2722 (1996).
- ³⁷B. I. Shklovskii and A. L. Efros, *Electronic Properties of Doped Semiconductors* (Springer, New York, 1984), pp. 297–299.